Supplementary data for

# Development of a Wireless-Controlled LED Array for the Tunable Optogenetic Control of Cellular Activities

Yuankai Qi [a,#], Junye Chen [a,b,#], Xuechun Liu [a,#], Xiaoxu Zhou [a,#], Jiannan Fan [a], Ping Shentu [a], Olof Idevall-Hagren [c], Yingke Xu [a,*]

[a] *Department of Biomedical Engineering, Key Laboratory for Biomedical Engineering of Ministry of Education, Zhejiang Provincial Key Laboratory of Cardio-Cerebral Vascular Detection Technology and Medicinal Effectiveness Appraisal, Zhejiang University, Hangzhou 310027, China*

[b] *Department of Hepatobiliary and Pancreatic Surgery, The Second Affiliated Hospital, School of Medicine, Zhejiang University, Hangzhou 310009, China*

[c] *Department of Medical Cell Biology, Uppsala Biomedical Centre, Uppsala University, Uppsala 75123, Sweden*

[#] These authors contributed equally to this study.

* Corresponding author.

E-mail address: yingkexu@zju.edu.cn (Y. Xu)

## Materials and methods

### *1. Materials and DNA constructs*

The rabbit anti-total Akt, anti-phospho-Akt(473), anti-phospho-Akt(308), and mouse anti-GAPDH were purchased from Cell Signaling Technology (Danvers, MA, USA). Antibodies against rabbit immunoglobulin G (IgG) and mouse IgG conjugated with horseradish peroxidase (HRP) were purchased from Abcam (Cambridge, MA, USA). Amplex™ Red and Amplex™ UltraRed hydrogen peroxide/peroxidase assay kits were purchased from Molecular Probes (Life Technologies, Carlsbad, CA, USA). Common chemicals and reagents were purchased from Sigma-Aldrich, unless otherwise noted. HRP-GFP plasmid was generously provided by Dr. Derek Toomre (Yale University, New Haven, CT, USA), and plasmids encoding CIBN-CAAX, mCherry-CRY2-iSH2, and mCherry-CRY2-OCRL were generated as described previously [1,2].

### *2. Cell culture and transfection*

HeLa cells were cultured in high-glucose Dulbecco's modified Eagle's medium (DMEM, Life Technologies, Carlsbad, CA, USA) with 10% fetal bovine serum (Gibco, Gland Island, NY, USA) and 1% penicillin G/streptomycin. The cells were kept at 37 ℃ in a humidified 5% $CO_2$ incubator. Cells were transfected with indicated plasmids using Lipofectamine® 2000 (Life Technologies) or electroporated using the Nucleofector™ 2b Device (Lonza, Basel, Switzerland).

### *3. Biochemical methods*

Biochemistry experiments were performed as previously described [1,3]. In brief, cells were washed with phosphate-buffered saline and lysed in RIPA lysis buffer (25 mmol Ł$^{-1}$ Tris, pH 7.4, 150 mmol Ł$^{-1}$ NaCl, 1 mmol Ł$^{-1}$ EDTA, 1% Triton X-100) containing protease inhibitors (cOmplete; Roche, Indianapolis, IN, USA). Equal amounts of protein (quantified by BCA protein assays, Thermo Scientific, Rockford, IL, USA) in each sample were analyzed using SDS-PAGE and immunoblotting. Proteins were transferred to polyvinylidene difluoride membrane (Bio-Rad, Berkeley, CA, USA) and hybridized to an appropriate primary antibody and HRP-conjugated secondary antibody for subsequent detection with ECL (Millipore, Billerica, MA, USA). Densitometric analysis was performed with ImageJ (National Institutes of Health, Bethesda, MD, USA).

### *4. HRP secretion assay*

HeLa cells were electroporated with CIBN-CAAX, mCherry-CRY2-OCRL, and HRP-GFP constructs and cultured in a black 96-well cell culture plate (Thermo Fisher Scientific, Rockford, IL, USA). After 12 h of transfection, the culture medium was changed and the cells were exposed to different conditions of light-emitting diode (LED) illumination. The culture medium was collected at different time intervals and cells were lysed at the end of the experiments. The secreted HRP in the medium and the HRP expressed inside the cells were detected by Amplex™ Red and Amplex™ UltraRed hydrogen peroxide/peroxidase assay kits according to the manufacturer's instructions. The HRP secretion was quantitatively analyzed and normalized with interval HRP levels.

### *5. Statistics*

Unless otherwise indicated, all data were presented as the mean ± standard error of mean (SEM) and analyzed using a Student's *t*-test.

*6. Circuit board LED driver stage schematic*

The LED driver stage contains the hardware needed to control the intensity of the LEDs in response to signals from the microcontroller, and the LEDs themselves. The core of the LED driver stage is 74HC595. 74HC595 is a latched shift register controlled by RCLK and SCLK, where the serial data P1.0 (same port but different name in other drivers) is first loaded to an internal buffer register and copied to output upon receipt of a load signal. All internal triggers are edge-triggered at a clock frequency of 33 MHz. Each input bit makes its way down to the *N*th output after *N* clock cycles, leading to parallel output. These chips are used as an expanded I/O port of the central processing unit (CPU) and are used to convert the input serial data into parallel format in order to control the LEDs individually. Each 74HC595 is connected to the microcontroller, and 8 LEDs are in series; thus, 12 of them were used in the 96-well cell culture plate format LED array. Only one of these drivers is shown in Fig. S1. The driver receives power from 5 V $V_{CC}$. A decoupling capacitor was included for each driver chip. The cathodes of the LEDs were connected to one of the output pins of the driver, and the anodes were connected to a chip resistor to $V_{CC}$. The sink current for each channel of 74HC595 is the same, making it possible for the LEDs to have the same light intensity.

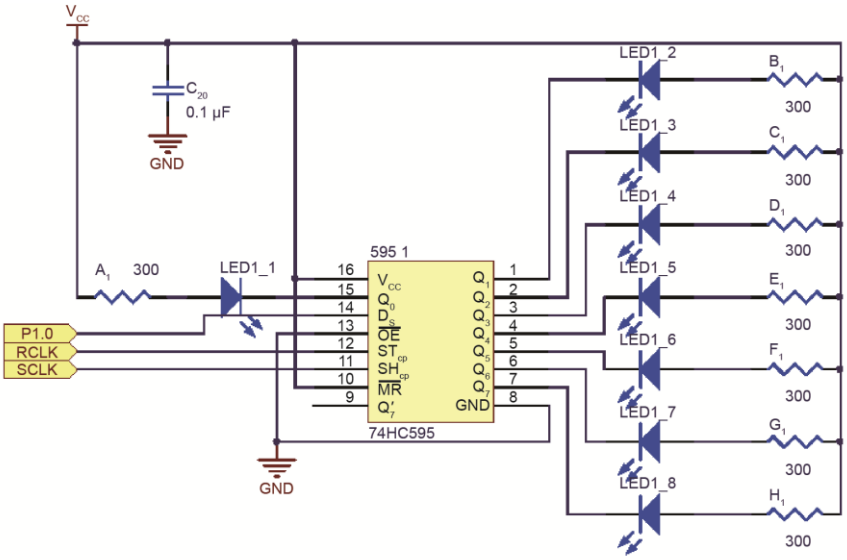


**Fig. S1.** Schematic of LED driver circuit board.

*7. Pulse-width modulation*

Pulse-width modulation (PWM) achieves the control of analog circuit frequency and amplitude by switching the inverter circuit on or off. The PWM output waveform is a series of square wave pulses of equal amplitude (Fig. S2).

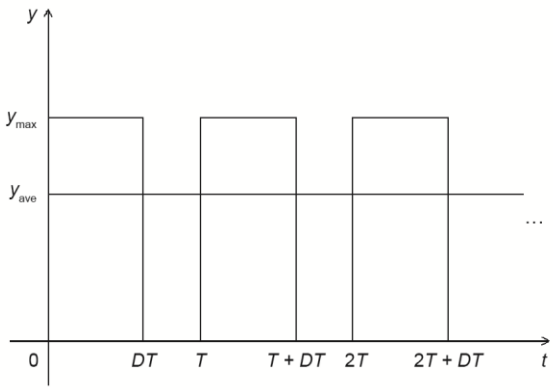


**Fig. S2.** Diagram of pulse-width modulation for the control of LEDs.

The average output value of the PWM waveform in a single period can be given by the following:

$$y = \frac{1}{T}\int_0^T f(t)\,\mathrm{d}t \qquad (1)$$

where $f(t)$ is the modulated square wave pulse of which the amplitude is $y_{max}$ when on ($nT < t < nDT$) and $y_{min}$ when off ($nDT < t < (n + 1)T$); thus, the formula above becomes:

$$\begin{aligned} y &= \frac{1}{T}\left(\int_0^{DT} y_{\max}\,\mathrm{d}t + \int_{DT}^{T} y_{\min}\,\mathrm{d}t\right) \\ &= \frac{1}{T}\left[y_{\max}\cdot DT + y_{\min}\cdot(1-D)T\right] \qquad (2) \\ &= y_{\max}\cdot D + y_{\min}\cdot(1-D) \end{aligned}$$

where $D$ is the duty cycle ($0 < D < 100\%$, expressed in percent) describing the proportion of "on" time to the regular interval or period, $T$. In our example, $y_{min}$ is zero, so the output only depends on $y_{max}$ and $D$. The main advantage of PWM is that power loss in the device is very low; it also works well with digital controls because of their on/off nature, and it is easy to set the necessary duty cycle to control the working voltage and brightness of the LEDs.

*8. Wireless light-control software*

The light-control software was developed on Visual Studio 2015 C# and Microsoft.NET framework 4.5. There are 8 ×12 panels, one for each LED; the intensity and illumination duration of each can easily be adjusted on the program. The software we developed has a user-friendly interface. The progress of the light-illumination experiments can be estimated and visualized in real time on the program interface (Fig. S3).

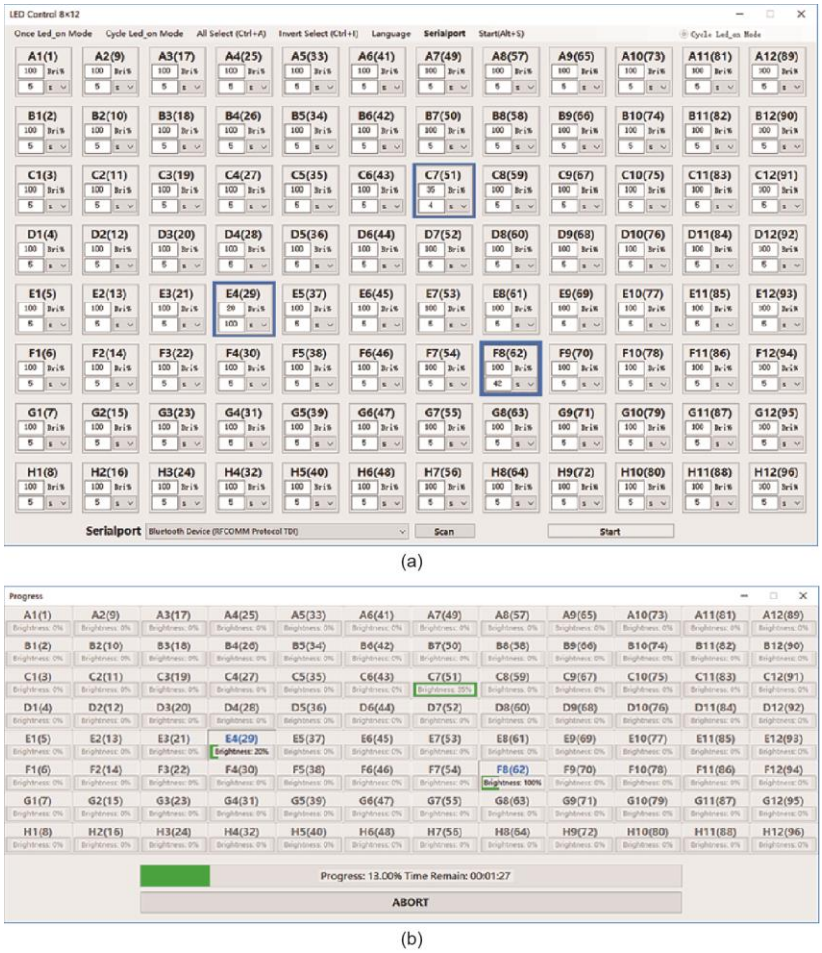


**Fig. S3.** Custom-developed software with user-friendly interface. (a) The main interface of the software was shown, which illustrates an example in which three LEDs were selected for light illumination; (b) visualized the progress of the experiment on the software interface.

*9. Advanced modes for controlling LED illumination*

The parameters for the modes of LED illumination can be exported and saved as Excel files (.xls), or can be loaded again from saved Excel files for the next experiment. The parameters can easily be modified directly on Excel files and be imported to the software. The software has a user-friendly interface that was designed to allow researchers to conveniently set or modify the parameters and reduce the duplication of work. The control software will point out the format error of parameters in loaded Excel files, including the type and location of the errors.

The parameters in the Once LED_on Mode are the number of LEDs selected, brightness, and LED on time (right panel of Fig. S4). The parameters in the Cycle LED_on Mode are the number of LEDs selected, brightness, LED on time, LED off time, and cycle/repeated times (left panel of Fig. S4). In the Advanced mode, it is possible to modify the parameters and set up the LEDs for more complicated illumination.

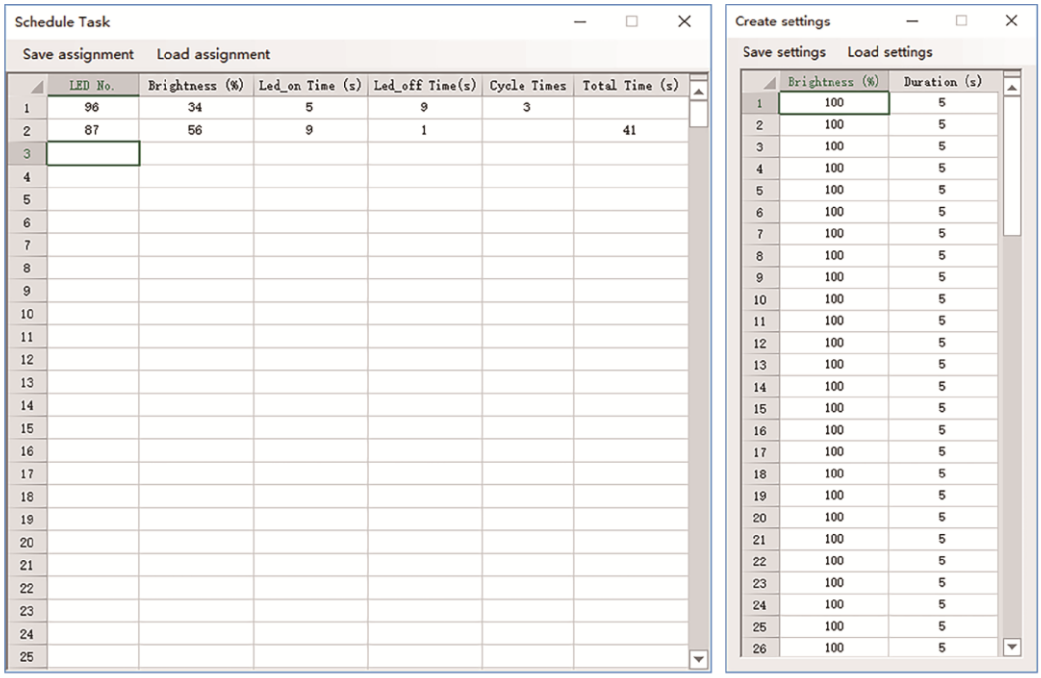


**Fig. S4.** The parameters for controlling of LEDs. The brightness, LED on/off times and cycles of light illumination can be adjusted for individual LEDs (left panel). The parameters can be easily modified on Excel format (right panel).

*10. Phototoxicity experiments*

To demonstrate whether the blue-light LEDs caused phototoxicity in the HeLa cells, we performed additional control experiments. We transfected HeLa cells with HRP constructs and divided the same batch of cells into four groups. The control cells were not exposed to blue-light LEDs; the other three groups were illuminated with 1% (0.6 mW), 5% (3 mW), and 10% (6 mW) of blue light, respectively. After 12 h of light illumination, we measured the quantity of HRP secretion and plotted the results in Fig. S5.

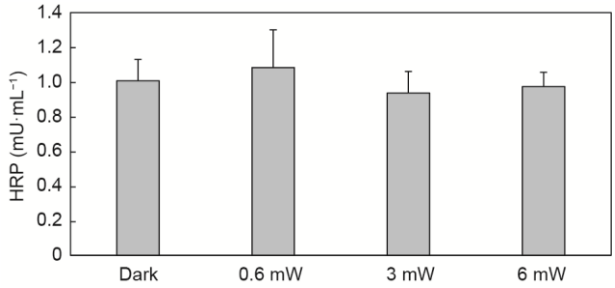


**Fig. S5.** Long-term blue-light LED illumination had negligible effect on HRP-GFP secretion from HeLa cells. HeLa cells were transfected with HRP-GFP. Then, the cells were illuminated with or without different doses of blue-light LED for 12 h. HRP secretion was quantified and plotted.

The results show that there are no statistic significant differences in HRP secretion between cells exposed to different doses of light and cells not exposed to light ($P > 0.05$). Furthermore, we did not detect cell death or the detachment of cells during the experiments. Thus, this experiment clearly showed that the effect of the blue light on cells is negligible, and that it does not affect the interpretation of the experimental results.

## References


[1] Xu Y, Nan D, Fan J, Bogan JS, Toomre D. Optogenetic activation reveals distinct roles of PI$P_3$ and Akt in adipocyte insulin action. J Cell Sci 2016;129(10):2085–95.
[2] Idevall-Hagren O, Dickson EJ, Hille B, Toomre DK, De Camilli P. Optogenetic control of phosphoinositide metabolism. Proc Natl Acad Sci USA 2012;109(35):E2316–23.
[3] Xu Y, Rubin BR, Orme CM, Karpikov A, Yu C, Bogan JS, et al. Dual-mode of insulin action controls GLUT4 vesicle exocytosis. J Cell Biol 2011;193(4):643–53.